Anesthesiology 2008; 109:436–47

Physicochemical Properties, Pharmacokinetics, and Pharmacodynamics of a Reformulated Microemulsion Propofol in Rats

Eun-Ho Lee, M.D., Soo-Han Lee, Ph.D.,† Do-Yang Park, A.S.,‡ Kyoung-Ho Ki, B.S.,‡ Eun-Kyung Lee, Ph.D.,† Dong-Ho Lee, M.D.,§ Gyu-Jeong Noh, M.D.,‖*

Background: **A newly developed microemulsion propofol consisted of 10% purified poloxamer 188 and 0.7% polyethylene glycol 660 hydroxystearate. The authors studied the physicochemical properties, aqueous free propofol concentration, and plasma bradykinin generation. Pharmacokinetics and pharmacodynamics were also evaluated in rats.**

Methods: **The pH, particle size, and osmolarity of microemulsion propofol were measured using a pH meter, particle size analyzer, and cryoscopic osmometer, respectively. The aqueous free propofol and plasma bradykinin were measured by a dialysis method and radioimmunoassay, respectively. Microemulsion propofol was administered by zero-order infusion of 0.5, 1.0, and 1.5 mg · kg^{-1} · min^{-1} for 20 min in 30 rats. The electroencephalographic approximate entropy was used as a surrogate measure of propofol effect.**

Results: **The pH, osmolarity, and particle size of microemulsion propofol are 7.5, 280 mOsm/l, and 67.0 ± 28.5 nm, respectively. The aqueous free propofol concentration in microemulsion propofol was 63.3 ± 1.2 μg/ml. When mixed with human blood, microemulsion propofol did not generate bradykinin in plasma. Although microemulsion propofol had nonlinear pharmacokinetics, a two-compartment model with linear pharmacokinetics best described the time course of the propofol concentration as follows: V_1 = 0.143 l/kg, k_{10} = 0.175 min^{-1}, k_{12} = 0.126 min^{-1}, k_{21} = 0.043 min^{-1}. The pharmacodynamic parameters in a sigmoid E_{max} model were as follows: E_0 = 1.18, E_{max} = 0.636, Ce_{50} = 1.87 μg/ml, γ = 1.28, k_{e0} = 1.02 min^{-1}.**

Conclusions: **Microemulsion propofol produced a high concentration of free propofol in the aqueous phase. For the applied dose range, microemulsion propofol showed nonlinear pharmacokinetics.**

* Clinical Assistant Professor, Department of Anesthesiology and Pain Medicine, † Research Professor, ‡ Research Associate, Department of Clinical Pharmacology and Therapeutics, § Professor, Department of Clinical Pharmacology and Therapeutics and Department of Anesthesiology and Pain Medicine, ‖ Professor and Chairman, Department of Clinical Pharmacology and Therapeutics, and Professor, Department of Anesthesiology and Pain Medicine.

Received from the Department of Clinical Pharmacology and Therapeutics and the Department of Anesthesiology and Pain Medicine, Asan Medical Center, University of Ulsan College of Medicine, Seoul, Korea. Submitted for publication February 11, 2008. Accepted for publication May 13, 2008. Supported by grant No. 2008-456 from the Asan Institute for Life Sciences, Seoul, Korea, and grant No. 2007-0003 from the Industry Trust Research Service between the University of Ulsan College of Medicine and Daewon Pharmaceutical Co., Ltd., Seoul, Korea. Song T-W, Sohn S-I, Jee U-K, Park J-K, Kim T-S, Kwon G-Y, inventors; Daewon Pharmaceutical Co., Ltd., assignee. Composition for injection including propofol and method of preparing the same. PCT publication PCT/KR2007/005146. October 19, 2007. Drs. E.-H. Lee and S.-H. Lee contributed equally to this work.

Address correspondence to Dr. Noh: 388-1, Pungnap 2-dong, Songpa-gu, Seoul 138-736, Korea. nohgj@amc.seoul.kr.

Available at: http://ctep.cancer.gov/forms/CTCAEv3.pdf. Accessed April 12, 2008.

LONG chain triglyceride emulsion propofol (LCT) has been associated with a variety of drawbacks, including poor physical stability, rapid growth of microorganisms, hyperlipidemia, pancreatitis, and pain on injection.[1–4] In our previous study, microemulsion propofol containing polyethylene glycol 660 hydroxystearate and tetrahydrofurfuryl alcohol polyethylene glycol ether was bioequivalent to LCT propofol.[5] However, the maximum tolerated intravenous doses of polyethylene glycol 660 hydroxystearate and tetrahydrofurfuryl alcohol polyethylene glycol ether were approximately 8 g and 5 g in a day, respectively, which limits the maximum volume of the previous formulation to be infused in a day to approximately 100 ml (July 1, 2004, a phase 1 clinical trial to assess the pharmacokinetic/pharmacodynamic characteristics and safety/tolerability of tetrahydrofurfuryl alcohol polyethylene glycol ether and polyethylene glycol 660 hydroxystearate in healthy subjects, study No. 2004-0124, Kyun-Seop Bae, M.D. and Gyu-Jeong Noh, M.D., Asan Medical Center, Seoul, Korea). This volume is equivalent to 5 ampoules (20 ml per ampoule) of 1% propofol in a day. The adverse events to terminate this dose escalation study were drug eruptions of Common Terminology Criteria for Adverse Events version 3.0# grade 2 or higher. The previous microemulsion propofol was, therefore, reformulated with purified poloxamer 188 (PP188) as a nonionic block copolymer surfactant and polyethylene glycol 660 hydroxystearate as a nonionic surfactant. The maximum tolerated intravenous dose of PP188 is 2,960 mg^{-1} · kg^{-1} · day.[6]

A lipid-free propofol solution was shown to produce frequent and severe pain on injection, possibly due to high concentration of free propofol in the aqueous phase, even though several side effects related to LCT may be reduced or eliminated.[7] Since Scott *et al.*[8] speculated that propofol produces injection pain by affecting the enzymatic cascade, possibly the plasma kallikrein–kinin system, there have been two hypotheses that related plasma bradykinin generation either by propofol itself[7] or by lipid solvent[9] to propofol-induced pain. However, no study observed plasma bradykinin generation by propofol itself, and many studies indicated less injection pain with higher levels of lipid solvent in lipid emulsion propofol.[10–12] Therefore, we evaluated plasma bradykinin generation as well as free propofol concentration in the aqueous phase, using both lipid-free and lipid emulsion propofol. In addition, factors associated

with pain on injection also include intrinsic properties of a drug such as structure and concentration, type of excipients used, properties of the final formulation such as pH, temperature, drug concentration, injection volume, and osmolality, and the injection procedure itself.[13] Therefore, to better understand the factors related to injection pain with microemulsion propofol, physicochemical properties (pH, osmolarity, particle size), free propofol concentration in the aqueous phase, and plasma bradykinin generation should be evaluated.

In a previous study, pharmacokinetics of LCT propofol in rats were found to be nonlinear and were best described by a two-compartment model with Michaelis-Menten elimination.[14] However, the underlying mechanism of nonlinearity should be determined, not by saturation of hepatic metabolism, but by hepatic blood flow and hence cardiac output, because hepatic metabolism of propofol is flow limited.[15] On the other hand, a few electroencephalographic metrics, such as modified median frequency, spectral edge frequency, and approximate entropy (ApEn), were used to describe the effects of propofol on the central nervous system.[16] Of these measures, ApEn is known to be robust to artifacts[17] and to correlate strongly with anesthetic effect site concentrations.[18] In particular, ApEn showed good correlation with the burst suppression ratio at high anesthetic drug concentrations.[19]

The objectives of this study were to perform pharmacokinetic and pharmacodynamic analysis of the reformulated microemulsion in rats, and to evaluate this formulation in regard to factors hypothesized to be involved in propofol emulsion–induced pain: plasma bradykinin generation and the aqueous free propofol concentrations in the absence and presence of added drugs reducing propofol-induced pain.

Materials and Methods

The assessment of plasma bradykinin generation in healthy volunteers was approved by the Institutional Review Board (Asan Medical Center, Seoul, Korea), and written informed consent was obtained from all participants. The pharmacokinetic and pharmacodynamic analyses in rats were approved by the Institutional Animal Care and Use Committee of the Asan Institute for Life Sciences (Seoul, Korea).

Preparation of Microemulsion Propofol

The formula of microemulsion propofol was as follows: a mixture of 1% propofol, 10% PP188 (Daebong LS Co., LTD, Seoul, Korea), 0.7% polyethylene glycol 660 hydroxystearate (Solutol HS 15; BASF Company Ltd., Seoul, Korea), 1% glycerin, 0.0008% disodium ethylenediaminetetraacetic acid (EDTA), and 0.01% sodium ascorbate. Propofol was obtained from Clariant LSM Inc. (Viale Europa, Italy). PP188 is comprised of a single chain (block) of hydrophobic polyoxypropylene flanked by two chains (blocks) of hydrophilic polyoxyethylene.[6] Propofol in microemulsion propofol is surrounded by a corona of PP188 and polyethylene glycol 660 hydroxystearate and serves as the lipid oil core of the microemulsion. Oxidative process in microemulsion propofol resulted in propofol dimerization and microemulsion yellowing. Microemulsion yellowing is caused by the formation of propofol dimer quinone.[20] Sodium ascorbate and disodium EDTA can function as a water-soluble antioxidant and a chelating agent, respectively, which completely inhibit the oxidative process in microemulsion propofol, and hence microemulsion remained visibly white at all times.

Microemulsion propofol was prepared by dispersing propofol at 70°C in a solution of PP188 using a constant speed stirrer at 1,500 rpm. When propofol is dissolved, polyethylene glycol 660 hydroxystearate, glycerin, sodium EDTA, and sodium ascorbate were added. Microemulsion propofol contained in an ampoule was autoclaved for 20 min at 121°C.

Physicochemical Properties of Microemulsion Propofol

The pH, particle size, and osmolarity were measured using a pH meter (model 720A; Orion Research Inc., Boston, MA), particle size analyzer (ELS-Z2; Otsuka Electronics Co., Ltd., Osaka, Japan), and cryoscopic osmometer (Osmomat 030; Gonotec GmbH, Berlin, Germany), respectively.

Measurement of Free Propofol Concentrations

In this study, the LCT propofol used as a comparator was 1% Diprivan® (AstraZeneca, London, United Kingdom). As described in a previous study,[4] propofol preparations were dialyzed using a dialysis membrane (Dialysis tubing benzoylated®; Sigma-Aldrich Co., St. Louis, MO) with a cutoff molecular weight of approximately 3,500–4,000 Da. A solution of 2.25% (wt/vol) glycerin (LG household & Health Care, Seoul, Korea) in water was used as the release medium. Microemulsion and lipid emulsion propofol (5 ml) were prepared to measure the free propofol concentration in the aqueous phase of each formulation.

To evaluate whether agents that reduce propofol-induced pain decrease the free propofol concentration, six mixtures were prepared: 5.5 ml of each propofol formulation (5 ml) and 2% lidocaine (0.5 ml),[21] 5.2 ml of each propofol formulation (5 ml) and ketamine (10 mg in 0.2 ml),[22] 6 ml of each propofol formulation (5 ml) and metoclopramide (5 mg in 1 ml),[23] 7 ml of each propofol formulation (5 ml) and ondansetron (4 mg in 2 ml),[24] 7 ml of each propofol formulation and thiopental (50 mg in 2 ml),[25] and 5.4 ml of each propofol formulation (5 ml) and ephedrine (2 mg in 0.4 ml)[26] (n = 10). As

controls, 5.2, 5.4, 5.5, 6.0, and 7.0 ml of each propofol formulation (5 ml) and saline (containing similar volumes of saline as the corresponding pain-reducing agents) were prepared (n = 10).

All samples were transferred to a dialysis membrane bag, and release media was added to produce a total volume of 10 ml. After sealing with a closer, the bag was immersed in 40 ml release medium and shaken for 100 strokes per min at 20°C in a water bath for 24 h.

Free propofol concentrations were measured using high-performance liquid chromatography (Agilent 1100 series; Agilent Technologies, Inc., Santa Clara, CA) with a C18 column (Xterra RP18, 5 μm, 4.6 × 150 mm; Waters Corporation, Milford, MA) and a tetrahydrofuran–water mixture as the mobile phase. The flow rate was 0.7 ml/min, and components of the column effluent were monitored using an ultraviolet detector with the wavelength set at 275 nm. Intraassay precision values were less than 2.44%. Interassay precision values were less than 7.27% (within day) and 4.57% (between day), respectively. Intraassay accuracy values were 89.88–101.64%, whereas interassay accuracy values were 90.27–101.46% of the nominal value.

Assessment of Bradykinin Generation in Plasma by Radioimmunoassay

Six adult healthy volunteers (M:F = 5:1) aged 29–39 yr with no medical history or medication were enrolled in this experiment.

Seven plastic syringes were prepared to contain the following samples at room temperature: 1.5 ml saline, LCT propofol, 10% lipid solvent (Intralipid; Kabi Pharmacia AB, Stockholm, Sweden), microemulsion propofol, 10% PP188, 0.7% polyethylene glycol 660 hydroxystearate, and a mixture of other ingredients in microemulsion propofol minus propofol, PP188, and polyethylene glycol 660 hydroxystearate. Saline (1.5 ml) was used as the control.

A 20-gauge angiocatheter was placed in a vein of the antecubital area, and 3.5 ml venous blood aspirated over 10 s from the catheter using prepared syringes. All samples were transferred to plain tubes containing 0.5 ml inhibition solution composed of aprotinin (10,000 KIU/ml), soybean trypsin inhibitor (800 μg/ml), and polybrene (4 mg/ml) for inactivation of plasma and glandular kallikrein and other kinin-producing enzymes, as well as 1,10-phenanthroline (10 mg/ml) and EDTA (20 mg/ml), for kinin-destroying enzymes.[27] Using this inhibition solution, bradykinin generation by propofol formulations and their components can be measured.

After shaking gently for 20 s, samples were centrifuged at 1,600*g* for 15 min at 4°C. The plasma was collected and stored at −70°C until assay.[20] The procedure for the extraction of peptides from plasma is described as follows: plasma (2 ml) was acidified with an equal amount of buffer A (1% trifluoroacetic acid; Sigma-Aldrich, Inc., St. Louis, MO), and centrifuged at 15,000*g* for 20 min at 4°C. The supernatant was loaded on to the pretreated separation column (Strata C18-E; Phenomenex, Inc., Torrance, CA), which was slowly washed with buffer A (3 ml, twice). The peptide was slowly eluted with 3 ml buffer B (buffer A containing 60% acetonitrile; Fisher Scientific, Pittsburgh, PA), and the eluent was collected in a polypropylene tube. The organic layer in the eluent was removed using a centrifugal concentrator (Savant Speedvac SPD2010; Thermo Fisher Scientific, Inc., Waltham, MA) for 15 min, and the remaining sample was subjected to freeze-drying overnight using a lyophilizer (Freeze Dry System; Labconco Corporation, Kansas City, MO).

The bradykinin concentration in samples was measured with a radioimmunoassay kit (Phoenix Pharmaceuticals, Inc., Burlingame, CA). Standard peptide was reconstituted with radioimmunoassay buffer provided by the manufacturer. Concentrated (lyophilized) bradykinin powder was dissolved in 250 μl radioimmunoassay buffer, and divided into 100-μl portions in duplicate. Appropriate dilutions of standard peptides (1,280, 640, 320, 160, 80, 40, 20, and 10 pg/ml) were used to generate a standard curve and were assayed in quadruplicate. Aliquot samples were assayed in duplicate. Assays were performed in 12 × 75-mm polystyrene tubes. After the addition of primary antibody, each tube was vortexed and incubated for 16–24 h at 4°C. Next, ^{125}I-peptide was added to each tube, and the procedure was repeated. Goat anti-rabbit immunoglobulin G and normal rabbit serum were added to each tube, vortexed, and incubated at room temperature for 90 min. Radioimmunoassay buffer was added and centrifuged at 1,700*g* for 20 min after gentle vortexing. The supernatant was aspirated, and assay tubes evaluated as counts per minute using a gamma counter (Packard Cobra Gamma Counters, Downers Grove, IL). A standard curve ($r^2 \geq 0.993$) was obtained by plotting standard peptide concentrations and was used to determine the bradykinin concentration. The measured bradykinin level was converted into plasma bradykinin (pg/ml) using a factor of 8. Specifically, lyophilized powder was made from 2 ml plasma and dissolved into 250 μl radioimmunoassay buffer. In cases where the measured bradykinin concentration was above or below the range of the standard curve, samples were diluted or concentrated accordingly. The sensitivity level was 0.81 pg/ml, and coefficients of variation for the intraassay and interassay were 1.8–5.5% and 1.4–7.1%, respectively.

Pharmacokinetic and Pharmacodynamic Analysis in Rats

Animals. Thirty adult male Sprague-Dawley rats (weight: mean ± SD, 450.9 ± 57.9 g; range, 347–560 g) were included in the study. The rats were housed with a controlled light–dark cycle (light on between 6:00 AM and 6:00 PM), an ambient temperature of 21°–

22°C, and unlimited access to standard laboratory rat diet and water.

Instrumentation and Drug Administration. The animals were anesthetized with sevoflurane in 100% O_2 (2–3 vol%). A cannula for drug infusion was inserted into the right jugular vein and placed into the superior vena cava 0.5 cm above the right atrium. The cannula was tunneled under the pelt and externalized on the dorsal surface of the neck. The right femoral artery was cannulated to measure systemic arterial pressure and to collect blood samples. Tracheostomy was performed for artificial ventilation. For proper monitoring of the anesthetic status of rat, previous method was modified.[28,29] Briefly, electroencephalography was monitored over the lateral left parietal cortex (Ch 1) and dorsal hippocampus cortex (Ch 2). For this purpose, rats were placed in a stereotaxic frame (model 900; David Kopf Instruments, Tujunga, CA), four burr holes (1-mm diameter) were drilled into the skull, and electrodes (Bone Anchor Screw; Stoelting, Wood Dale, IL) were threaded as follows. One was placed midline in the frontal bone and used as a reference; one was placed midline in the occipital bone and used as a ground. One electrode per parietal bone was placed 3–5 mm lateral and 4–5 mm posterior to the bregma. For better electrical conduction between the dura and electrodes, the burr holes were filled with paste for electroencephalography (Elefix; Nihon Kohden, Tokyo, Japan). Electrodes were connected to commercial eight-pin serial computer connector, and the entire electrode and connector assembly was insulated and bonded to the skull with dental cement. Vecuronium (2 mg/kg) was administered intravenously to paralyze the animal. Then, the animal was artificially ventilated using a ventilator for small animals (Inspira ASV; Harvard Apparatus, Holliston, MA). The animal was placed in a supine position, and the head was extended and firmly immobilized in a stereotaxic frame. The electroencephalography connector was connected to the electroencephalography receiver and computer. Mean arterial pressures (MAPs) were continuously recorded from the arterial cannula using a patient monitor (Datex-Ohmeda S/5; Planar Systems, Inc., Beaverton, OR). Body temperature was monitored rectally and was maintained by a heating lamp. After the completion of initial instrumentation, an additional 1 h served as a stabilization period. Anesthesia was maintained with sevoflurane adjusted to keep MAP within ±15% of baseline values during the stabilization period. For 20 min before the administration of microemulsion propofol, sevoflurane was washed out. Depending on the raw electroencephalographic signal, sevoflurane was readministered after discontinuation of microemulsion propofol.

Blood gas analysis from an arterial sample was performed shortly before and approximately 20 min after administration of the study drug as well as at the end of the experiment.

The pharmacokinetics of microemulsion propofol were determined upon intravenous administration of 0.5, 1.0, and 1.5 $mg \cdot kg^{-1} \cdot min^{-1}$ (n = 10 at each dose) during 20 min. The microemulsion propofols were administered using an infusion pump (Pump 11 Pico Plus; Harvard Apparatus) and a Hamilton syringe (Hamilton Company, Reno, NV).

Blood Sample Acquisition and Drug Assay. For propofol analysis, arterial blood samples of 300 μl each were collected immediately before and at 2, 5, 7, 10, 15, 20, 30, 45, 60, and 90 min after administration. Samples were collected in heparinized tubes and were stored at −70°C until assay. Drawn blood was substituted by twice the volume of Hartman solution for maintenance of blood pressure.

Propofol was isolated from whole blood by extraction using pretreatment with deproteinization and was determined by high-performance liquid chromatography with fluorescence detection. Plasma proteins were precipitated with acetonitrile. The supernatants were analyzed by high-performance liquid chromatography using a Capcell Pak C18 UG120 column (Shiseido Fine Chemicals, Tokyo, Japan) and a mixture of acetonitrile and 0.1% trifluoroacetic acid in water (56:44, vol/vol) as a mobile phase. The components of the column effluent were monitored by a fluorometric detector with excitation and emission wavelengths set at 276 and 310 nm, respectively.

The lower limit of quantification of propofol was 50 ng/ml. The calibration curve was linear over the range of 50–5,000 ng/ml, with the coefficients of determination (R^2) greater than 0.999 for all cases. Intraassay precision values were less than 5.74%. Interassay within-day and between-day precision values were less than 3.65% and 9.33%, respectively. Intraassay accuracy values were 86.66–103.94% of the nominal value. Interassay accuracy values were 99.06–103.72% of the nominal value.

Noncompartmental Pharmacokinetic Analysis. Pharmacokinetic parameters were calculated by noncompartmental methods (WinNonlin Professional 5.2; Pharsight Corporation, Mountain View, CA). The area under the curve from the time of administration to the last measured concentration (AUC_{last}) was estimated by linear trapezoidal integration (linear interpolation). The area under the curve from administration to infinity (AUC_{inf}) was calculated as the sum of $AUC_{last} + C_{last}/\lambda_Z$, in which C_{last} is the last measured concentration and λ_Z is the apparent terminal rate constant estimated by unweighted linear regression for the linear portion of the terminal log concentration–time curve. The maximal concentration (C_{max}) and the time to reach C_{max} (t_{max}) after an intravenous infusion of microemulsion propofol were determined from the observed data. Summary statistics were determined for each parameter. To evaluate dose linearity, dose-normalized AUC_{inf} values among each dose group were compared using one-way analysis of variance (ANOVA).[30] If the differences among three

groups are statistically insignificant, we conclude that pharmacokinetics show dose linearity. In addition, we used a power model and confidence interval criteria approach as follows.[30]

$$PK = \beta_0 \cdot Dose^{\beta_1}, \quad (1)$$

where dose linearity implies that $\beta_1 = 1$ in equation 1 and PK denotes a pharmacokinetic variable.

Population Pharmacokinetic Analysis. One-, two-, and three-compartment models with linear pharmacokinetics were fitted using an ADVAN 6 subroutine and the first-order conditional estimation procedure of NONMEM® VI (GloboMax LLC, Ellicott City, MD). The interindividual random variability on each of the model parameters was modeled using a log-normal model. A diagonal matrix was estimated for the different distributions of ηs, where η is interindividual random variability with mean zero and variance ω^2. A constant coefficient of variation model was used for the residual random variability. In addition, the time course of the propofol concentration was modeled using nonlinear models with Michaelis-Menten elimination and the well-stirred model.[31] The latter is one of hepatic clearance models to describe hepatic elimination of drugs, in which drug concentration is assumed to be constant throughout the hepatic compartment and equal to the outflow concentration.

For Michaelis-Menten elimination, clearance is defined as follows:

$$Cl = V_{max}/(K_m + C), \quad (2)$$

where V_{max} is the maximum metabolic rate and K_m is the Michaelis-Menten constant in equation 2.

For the well-stirred model,

$$Cl_H = (Q_H \cdot f_u \cdot Cl_{int})/(Q_H + f_u \cdot Cl_{int}), \quad (3)$$

where Cl_H is hepatic clearance, Q_H is hepatic perfusion rate, f_u is the free fraction of a drug, and Cl_{int} is intrinsic clearance in equation 3. For simplicity, we can denote $f_u \cdot Cl_{int}$ by Cl_{int}.

Electroencephalographic Analysis. The electroencephalographic activity of two-channel was continuously recorded by QEEG-8 (LXE3208; Laxtha Inc., Daejeon, Korea). The sampling frequency of the analyzed channel was 256 Hz. Baseline electroencephalographic activity was recorded for 5 min before continuous infusion of microemulsion propofol.

The raw electroencephalographic signal was filtered between 0.5 and 50 Hz for on-line calculation of the electroencephalographic approximate entropy (ApEn; Telescan version 2.85 and Complexity version 2.7; Laxtha Inc.) which quantifies the regularity of the data time series and is known to show better baseline stability as a measure of the arousal state of the central nervous system than other univariate descriptors.[17,32] To calculate ApEn, the length of the epoch (N) was 2,056, the number of previous values (m) used to predict the subsequent values was 2, and a filtering level (r) was 15% of the SD of the amplitude values. Smoothing by means of a simple moving average was applied to the calculation of ApEn. The number of neighboring points was seven. Serious artifacts were excluded by checking the maximum amplitude for each epoch; if the amplitude was greater than 200 μV, the epoch was excluded. The appropriateness of artifact rejection was manually confirmed. Artifact rejection and analysis of each electroencephalographic parameter were performed by a single, blinded, experienced analyst.

Population Pharmacodynamic Analysis. To account for the time lag (hysteresis) between the onset of the effect and the course of the plasma concentration, the pharmacodynamics were described using an effect compartment model in which k_{e0}, a first-order elimination rate constant characterizing effect site equilibration, was used to estimate the apparent effect site concentrations. For each animal, the relation of ApEn with propofol effect site concentration was analyzed using a sigmoid E_{max} model:

$$Effect = E_0 + (E_{max} - E_0)(Ce^{\gamma}/(Ce^{\gamma}_{50} + Ce^{\gamma})), \quad (4)$$

where Effect is ApEn, E_0 is the baseline ApEn when no drug is present, E_{max} is the ApEn value for maximum possible drug effect, Ce is the calculated effect site concentration of propofol, Ce_{50} is the effect site concentration associated with 50% maximal drug effect, and γ is the steepness of the concentration-*versus*-response relation in equation 4.

Interindividual random variability of Ce_{50} and k_{e0} was modeled using a log-normal model, and no interindividual variability of E_0, E_{max}, or γ was assumed. A diagonal matrix was estimated for the different distributions of ηs. Residual random variability was modeled using an additive error model.

Model Diagnosis and Validation. The models were evaluated using statistical and graphical methods. The minimal value of the objective function (equal to minus twice the log likelihood) provided by NONMEM® was used as the goodness-of-fit characteristic to discriminate between hierarchical models using the log likelihood ratio test.[33] A *P* value of 0.05, representing a decrease in objective function value of 3.84 points, was considered statistically significant (chi-square distribution, $df = 1$). R (version 2.6.1; R Foundation for Statistical Computing, Vienna, Austria) was used for graphical model diagnosis.

To compare the distribution of ηs to the normal distribution, we calculated the correlation of the points in the normal probability plot in which the null hypothesis of the test is that the data come from a normal distribution.[34,35] If we obtain a *P* value greater than 0.05, we fail

Table 1. Free Propofol Concentrations in the Aqueous Phase of Long Chain Triglyceride Emulsion Propofol (LCT Propofol) and Microemulsion Propofol with or without Agents Reducing Propofol-induced Pain

Agents Mixed with Propofol Formulations	LCT Propofol, μg/ml		Microemulsion Propofol, μg/ml	
	Control*	Added Drug†	Control*	Added Drug†
None‡	—	12.4 ± 0.7	—	63.3 ± 1.2
2% Lidocaine, 10 mg in 0.5 ml	12.3 ± 0.5	12.3 ± 0.6	63.4 ± 0.5	63.7 ± 0.7
Ketamine, 10 mg in 0.2 ml	12.4 (12.1, 12.5)	12.3 (11.6, 13.2)	63.5 ± 0.6	63.8 ± 0.5
Metoclopramide, 5 mg in 1 ml	12.2 ± 0.6	11.9 ± 0.6	63.4 ± 0.5	63.3 ± 0.3
Ondansetron, 4 mg in 2 ml	12.4 ± 0.7	12.5 ± 0.7	63.7 ± 0.6	63.5 ± 0.5
Thiopental, 50 mg in 2 ml	12.4 ± 0.7	12.2 ± 0.6	63.7 ± 0.6	63.3 ± 0.6
Ephedrine, 2 mg in 0.4 ml	12.3 ± 0.6	12.4 ± 0.7	63.6 ± 0.5	63.4 ± 0.5

n = 10 for every sample of control and test. Data are stated as mean ± SD or median (25%, 75%) and were analyzed by paired *t* test or Mann–Whitney rank sum test as appropriate.

* Mixture of each propofol formulation (5 ml) and saline (0.2, 0.4, 0.5, 1.0, and 2.0 ml, respectively). The volume of saline mixed was equal to that of pain-reducing agent in a corresponding test. † Mixtures of each propofol formulation (5 ml) and pain-reducing agents (the volume of each agent is indicated in parenthesis). ‡ The free propofol concentrations in the aqueous phase of long chain triglyceride (LCT) propofol and microemulsion propofol were compared ($P < 0.001$). Otherwise, control and test samples in each propofol formulation were compared to test the effects of agents known to reduce propofol-induced pain on the free propofol concentrations in the aqueous phase ($P > 0.05$ for all pairwise comparisons).

to reject the null hypothesis and conclude that normality is a reasonable assumption.

The weighted residual was calculated as (measured − predicted)/predicted. The median weighted residual and median absolute weighted residual were calculated to examine the quality of the prediction of the pharmacokinetic models for the population. We used the median absolute residual and its percentage of pharmacodynamic range ($E_0 - E_{max}$) of the final model to describe the quality of prediction for the population.

For both the final pharmacokinetic and pharmacodynamic models, a nonparametric bootstrap analysis was performed as an internal model validation, using the software package Wings for NONMEM® VI (Holford N, version 600; Auckland, New Zealand).[36] This process was repeated 2,000 times. The final model parameter estimates were compared with the median parameter values and with the 2.5–97.5 percentile of the nonparametric bootstrap replicates of the final model.

Statistical Analysis

The statistical analyses were performed with SPSS (version 12.0; SPSS Inc., Chicago, IL). The concentrations of free propofol in the aqueous phase in microemulsion and LCT propofol were analyzed using a *t* test or Mann–Whitney rank sum test, as appropriate. Differences in measured concentrations of bradykinin in plasma between the groups were compared using one-way ANOVA. Changes in blood pressure were tested for statistical significance using repeated-measures ANOVA and the Tukey *post hoc* test. Baseline (E_0) and maximally decreased ApEn (E_{max}) and the difference between E_0 and E_{max} values of the lateral left parietal cortex and dorsal hippocampus cortex were compared using a *t* test or Mann–Whitney rank sum test, as appropriate. E_0 and E_{max} and the difference between E_0 and E_{max} values among each infusion rate were compared using one-way ANOVA or Kruskal–Wallis one-way ANOVA on ranks, as appropriate. In all comparisons, a *P* value less than 0.05 was considered statistically significant. Data are the mean ± SD unless stated otherwise.

Results

Physicochemical Properties of Microemulsion Propofol

The pH, osmolarity, and particle size of microemulsion propofol were 7.5, 280 mOsm/l, and 67.0 ± 28.5 nm, respectively.

Measurement of Free Propofol Concentrations

The free propofol concentrations in the aqueous phase of LCT propofol and microemulsion propofol with or without agents reducing propofol-induced pain are shown in table 1. The aqueous free propofol concentration of microemulsion propofol was five times higher than that of LCT propofol, suggesting the possibility of more severe and frequent pain on injection. Notably, no agents showed any influence on the level of the aqueous free propofol in either formulation.

Assessment of Bradykinin Generation in Plasma by Radioimmunoassay

Plasma bradykinin concentrations when LCT propofol and microemulsion propofol and their components were mixed with human blood are shown in figure 1. No significant differences among all agents used in this experiment were observed, which is contradictory to other studies.[37,38] These findings suggest that bradykinin generation induced by contact of both formulations with plasma may not be associated with injection pain.

Hemodynamics

Changes of MAP over time for all animals are shown in figure 2. MAP decreased significantly at the infusion rates

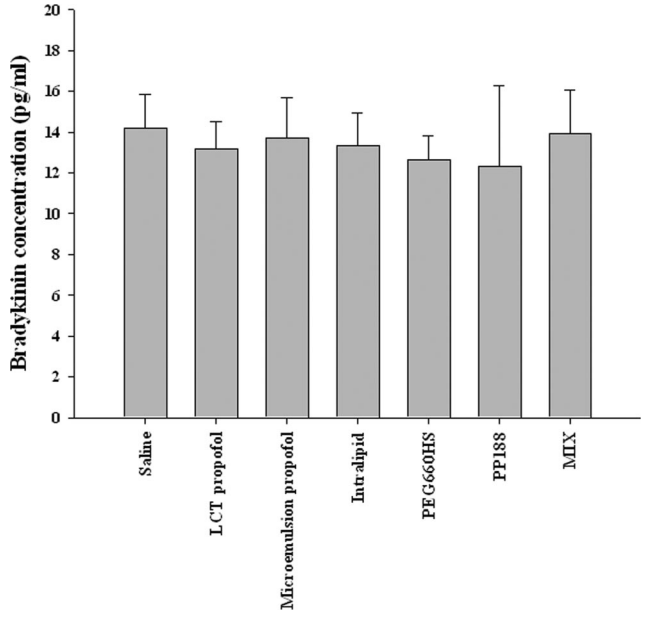

Fig. 1. Plasma bradykinin concentrations when long chain triglyceride emulsion propofol (LCT propofol) and microemulsion propofol and their components were mixed with human blood. MIX = mixture of other ingredients in microemulsion propofol minus propofol, PP188, and PEG660HS; PEG660HS = 0.7% polyethylene glycol 660 hydroxystearate; PP188 = 10% purified poloxamer 188.

of 1.0 and 1.5 mg · kg^{-1} · min^{-1}, compared with baseline MAPs and those at the infusion rate of 0.5 mg · kg^{-1} · min^{-1}. MAP at the infusion rates of 1.0 and 1.5 mg · kg^{-1} · min^{-1} was recovered to baseline values approximately 90 min after start of infusion. However, MAP between 1.0 and 1.5 mg · kg^{-1} · min^{-1} at each time point did not show statistically significant difference. The SD of MAP at each time point ranged from 9.2 to 16.4 mmHg for 0.5 mg · kg^{-1} · min^{-1}, from 13.2 to 30.3 mmHg for 1.0 mg · kg^{-1} · min^{-1}, and from 8.3 to 27.8 mmHg for 1.5 mg · kg^{-1} · min^{-1}, suggesting large interindividual variability of MAP at the infusion rates of 1.0 and 1.5 mg · kg^{-1} · min^{-1}. Normocapnia (arterial carbon dioxide tension = 35.5 ± 6.6 mmHg) and normothermia (36.5° ± 0.4°C) were maintained throughout the study period.

Pharmacokinetic and Pharmacodynamic Analysis

The infusion of microemulsion propofol was started 244.1 ± 47.3 min after the beginning of the surgical preparation. The time course of the propofol concentration is illustrated in figure 3.

Noncompartmental Pharmacokinetic Analysis. In all animals, at least 80% of the total area under the curve was covered by measured concentrations. Table 2 shows the pharmacokinetic parameters that are calculated by noncompartmental methods. The relation between the total dose and the total area under the curve after log transformation is presented in figure 4 and revealed dose nonlinearity. These nonlinear pharmacokinetics were also evidenced by the finding that the areas under the plasma concentration–time curve from time 0 to infinity normalized by dose (AUC_{inf}/dose) for the infusion rates of 0.5, 1.0, and 1.5 mg · kg^{-1} · min^{-1} were 29.9 ± 8.4, 48.6 ± 15.8, and 52.1 ± 10.2 min · μg · ml^{-1} · mg^{-1}, respectively ($P < 0.001$).

Population Pharmacokinetic Analysis. For microemulsion propofol, the decline of the plasma concentration was biphasic, with an initial fast decline and a slower terminal elimination. A two-compartment model best described the time course of the propofol concentration, whereas nonlinear models with Michaelis-Menten elimination and the well-stirred model were not successful to be fitted to the pharmacokinetic data. We

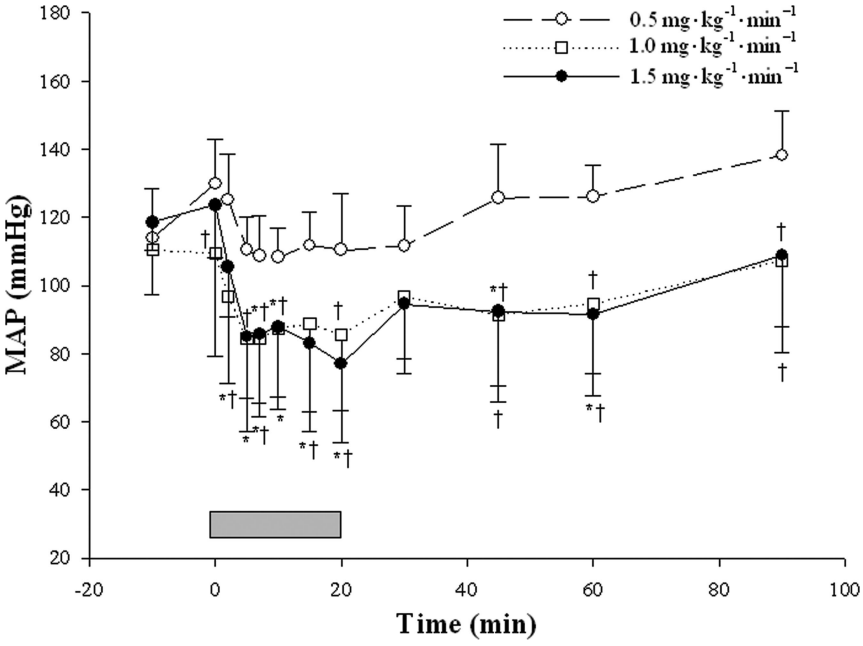

Fig. 2. Changes of mean arterial pressure (MAP) over time for all rats. Data are stated as mean ± SD. The *gray bar* at the bottom indicates infusion of microemulsion propofol. *Open circles* = MAP at 0.5 mg · kg^{-1} · min^{-1}; *open squares* = MAP at 1.0 mg · kg^{-1} · min^{-1}; *solid circles* = MAP at 1.5 mg · kg^{-1} · min^{-1}. * $P < 0.05$ *versus* baseline. † $P < 0.05$ *versus* 0.5 mg · kg^{-1} · min^{-1}.

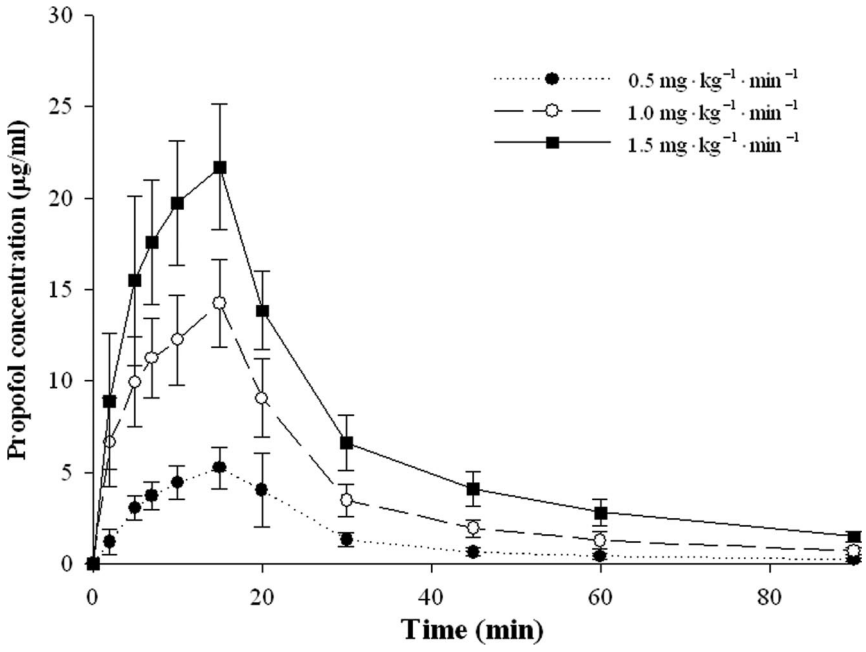

Fig. 3. Propofol concentrations over time during and after infusion of microemulsion propofol in rats. Data are stated as mean ± SD. *Solid circles* = mean plasma propofol concentrations at 0.5 mg · kg^{-1} · min^{-1}; *open circles* = mean plasma propofol concentrations at 1.0 mg · kg^{-1} · min^{-1}; *solid squares* = mean plasma propofol concentrations at 1.5 mg · kg^{-1} · min^{-1}.

also tried to include MAP as a time varying covariate for CL1 in table 3 but did not show statistical significance despite successful minimization. This might be attributed to large SDs of MAP, particularly at the infusion rates of 1.0 and 1.5 mg · kg^{-1} · min^{-1}. Table 3 summarizes the results of the final population pharmacokinetic model. All of the ηs except η for k_{10} and k_{12} were normally distributed. Measured and predicted concentrations of propofol over time are depicted in figure 5.

Population Pharmacodynamic Analysis. The stability of baseline (E_0) and maximally decreased ApEn (E_{max}) and the difference between E_0 and E_{max} values of the lateral left parietal cortex and dorsal hippocampus cortex (both referenced by frontal cortex) in rats are shown in table 4. The overall baseline stability and the overall difference between E_0 and E_{max} of the lateral left parietal cortex were better and larger than those of dorsal hippocampus cortex, respectively. Especially the difference between E_0 and E_{max} values of the lateral left parietal cortex tended to increase more consistently in a dose-dependent manner. Therefore, ApEn derived from the lateral left parietal cortex (Ch 1) was chosen for pharmacodynamic modeling. The time course of the electroencephalographic entropy (ApEn) derived from the lateral left parietal cortex during and after the infusion of microemulsion propofol in rats is shown in figure 6.

Estimates of the population parameters of the final pharmacodynamic model for microemulsion propofol are summarized in table 5. The equilibration half-life, $t_{1/2ke0}$, was approximately 0.68 min. The ηs of Ce_{50} and k_{e0} in the final pharmacodynamic model were normally distributed. Observed and predicted ApEn values over time are shown in figure 7.

Table 2. Noncompartmental Pharmacokinetic Parameters of Microemulsion Propofol after an Intravenous Infusion for 20 Minutes

	Infusion Rate		
	0.5 mg · kg^{-1} · min^{-1}	1.0 mg · kg^{-1} · min^{-1}	1.5 mg · kg^{-1} · min^{-1}
λ_Z, min^{-1}	0.0223 ± 0.0027	0.0247 ± 0.0039	0.0223 ± 0.0025
t_{max}, min	16 ± 2	15	14 ± 3
C_{max}, μg/ml	5.4 ± 1.4	14.2 ± 2.4	21.7 ± 3.4
AUC_{last}, min · μg · ml^{-1}	133.5 ± 39.0	369.5 ± 82.1	625.5 ± 105.3
AUC_{inf}, min · μg · ml^{-1}	144.2 ± 41.7	398.7 ± 90.3	692.6 ± 114.9
$AUC_{\%Extrap}$, %	7.4 ± 1.5	7.3 ± 1.1	9.7 ± 1.4
V_z, ml/kg	3,388.6 ± 992.9	2,143.2 ± 484.3	2,040.8 ± 566.7
Cl, ml · min^{-1} · kg^{-1}	74.5 ± 20.8	52.3 ± 10.7	44.6 ± 8.8
MRT_{last}, min	13 ± 1	13 ± 1	16 ± 1
V_{ss}, ml/kg	1,584.4 ± 385.7	1,088.0 ± 213.0	1,174.2 ± 252.2

$AUC_{\%Extrap}$ = percentage of the extrapolated area under the curve at the total area under the curve; AUC_{inf} = area under the curve from administration to infinity; AUC_{last} = area under the curve from administration to the last measured concentration; C_{max} = maximal concentration; λ_Z = terminal elimination rate constant; MRT_{last} = mean residence time of the drug in the body; t_{max} = time at maximal concentration; V_{ss} = volume of distribution at steady state; V_z = volume of distribution.

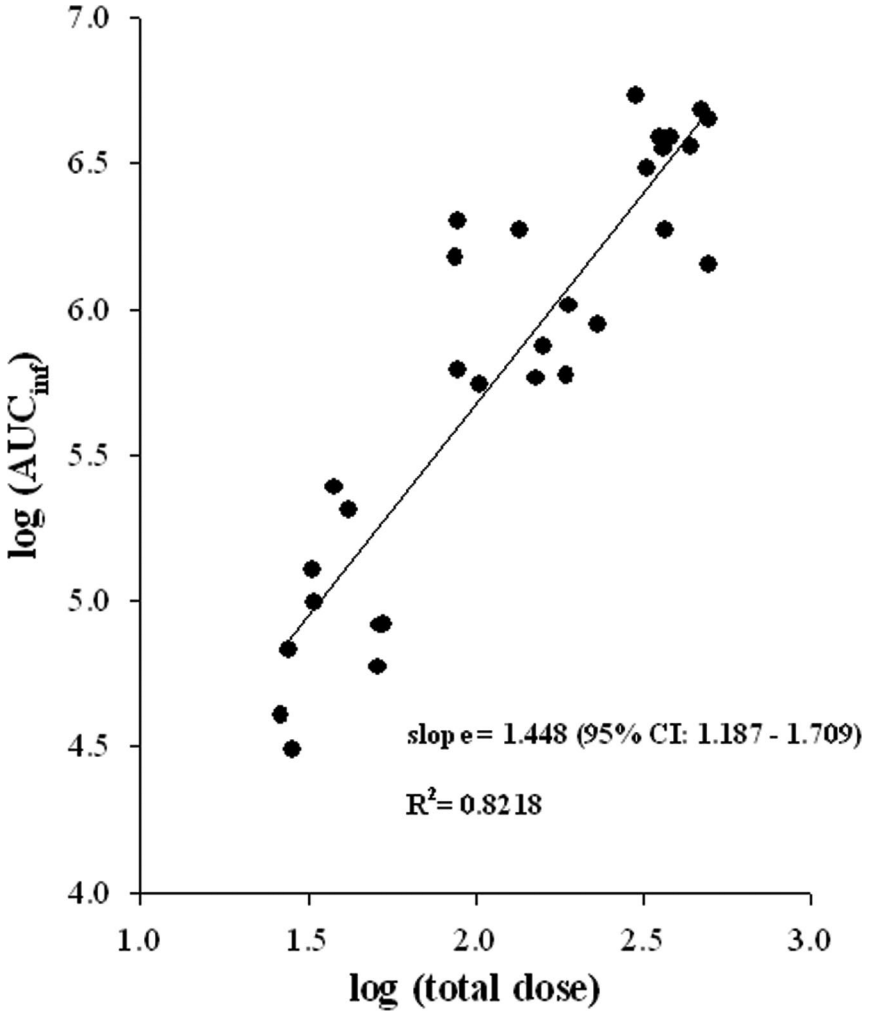

Fig. 4. The relation between area under the curve from administration to infinity (AUC_{inf}; min · μg/ml) and the total dose (milligrams) of microemulsion propofol after log transformation. The slope is not equal to 1, which suggests nonlinearity. CI = confidence interval.

Discussion

Free propofol concentration in the aqueous phase of the reformulated microemulsion propofol was five times higher than those of LCT propofol. Both formulations and their components did not generate bradykinin in plasma on mixing with human blood. Our *in vitro* studies provide the evidence that both free propofol and lipid solvent do not activate the plasma kallikrein–kinin system and lipid solvent in LCT propofol decreases free

Table 3. Population Pharmacokinetic Parameter Estimates (RSE) and Interindividual Variability (%CV) and Median Parameter Values (2.5–97.5%) of the Nonparametric Bootstrap Replicates of the Final Pharmacokinetic Model of a Reformulated Microemulsion Propofol

Parameter	Estimate (RSE, %CV)	Median	2.5–97.5%
V1, θ1, l/kg	0.143 (12.59, 62.4)	0.142	0.11–0.183
V2, θ2, l/kg	0.422 (4.98, –)	0.423	0.387–0.464
CL1, θ3, l · kg^{-1} · min^{-1}	0.025 (6.2, 33.8)	0.0248	0.0222–0.028
CL2, θ4, l · kg^{-1} · min^{-1}	0.018 (3.69, –)	0.0176	0.0163–0.0189
σ^2	0.036 (7.36, –)	0.0359	0.0314–0.0414

Interindividual random variability and residual random variability were modeled using log-normal model and constant coefficient of variation model, respectively. Nonparametric bootstrap analysis was repeated 2,000 times.

CV = coefficient of variation; σ^2 = variance of residual random variability; RSE = relative standard error.

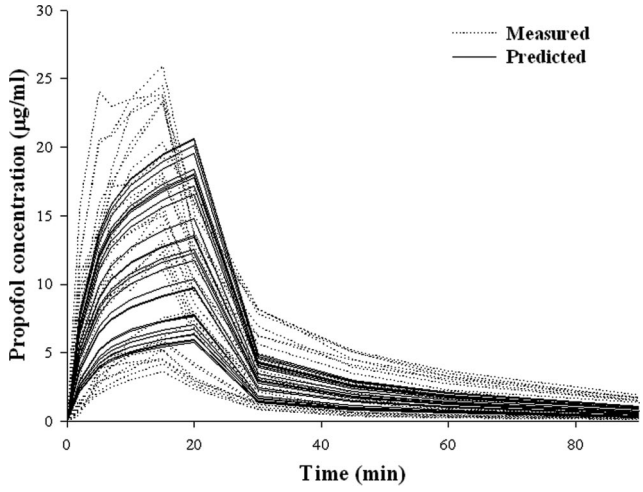

Fig. 5. Measured (*dotted lines*) and predicted (*solid lines*) concentrations of propofol over time. The median weighted residual and median absolute weighted residual of the pharmacokinetic model were −1.9% and 27%, respectively.

Table 4. Stability of Baseline (E_0) and Maximally Decreased Approximate Entropy (E_{max}), and Difference between E_0 and E_{max} Values of Lateral Left Parietal Cortex and Dorsal Hippocampus Cortex in Rats

Parameter	Infusion Rates of Microemulsion Propofol, mg · kg^{-1} · min^{-1}	Lateral Left Parietal Cortex	Dorsal Hippocampus Cortex
E_0, CV% (mean ± SD)	Overall	12.1 (1.090 ± 0.132)*	12.7 (0.978 ± 0.124)
	0.5	8.7 (1.130 ± 0.099)	9.7 (1.041 ± 0.101)
	1.0	18.0 (1.029 ± 0.185)	14.4 (1.090 ± 0.132)
	1.5	6.8 (1.090 ± 0.132)*	12.1 (0.928 ± 0.134)
E_{max}, CV% (mean ± SD)	Overall	12.0 (0.688 ± 0.083)	13.9 (0.676 ± 0.094)
	0.5	5.5 (0.772 ± 0.042)†	8.0 (0.772 ± 0.061)†
	1.0	9.9 (0.660 ± 0.065)†	5.6 (0.669 ± 0.037)†
	1.5	9.3 (0.631 ± 0.059)†	10.9 (0.587 ± 0.064)†
$E_0 - E_{max}$, mean ± SD (CV%)	Overall	0.402 ± 0.126* (31.3)	0.302 ± 0.130 (43.0)
	0.5	0.358 ± 0.077*† (21.5)	0.269 ± 0.090 (33.3)
	1.0	0.369 ± 0.148† (40.1)	0.259 ± 0.138 (53.3)
	1.5	0.480 ± 0.114† (23.8)	0.379 ± 0.133 (35.1)

* $P < 0.05$ *vs.* dorsal hippocampus cortex. † $P < 0.05$ comparison among each infusion rate.
CV = coefficient of variation.

propofol concentration in the aqueous phase, and hence plays an important role in decreasing propofol-induced pain. Injection pain of a number of sedative and hypnotic drugs is possibly caused by formulations of extremely unphysiologic osmolality.[39] Because the pH and osmolarity/osmolality of microemulsion and lipid emulsion are almost within physiologic ranges (pH 6–8.5 and 0.303 Osm/kg for lipid emulsion propofol[40]), these factors are unlikely to cause injection pain. Therefore, propofol-induced pain may be attributed to the direct irritation of free nerve endings by free propofol in the aqueous phase.

The exact mechanism of action of lidocaine, ketamine, metoclopramide, ondansetron, thiopental, and ephedrine reducing propofol-induced pain is still unclear. In this study, the mixtures of LCT propofol and microemulsion propofol with these agents neither decreased nor increased the level of free propofol in the aqueous phase. Considering this result as well as plasma bradykinin study, these agents may act *via* local effects to reduce the irritation effect of free propofol.

In a previous study, the central volume of distribution (V_c) and the volume of distribution at steady state (V_{ss}) of LCT propofol were 0.13 and 0.8 l/kg, respectively.[14] Compared with these results, microemulsion propofol showed similar V_c (0.143 l/kg) but slightly smaller V_{ss} (0.565 l/kg), which may be due to the influence of formulation on the pharmacokinetics of propofol or a different infusion scheme as well as a different sampling schedule. Despite differences in contents, the formulation effect on the pharmacokinetics of propofol was also demonstrated in our previous study in which microemulsion propofol may be less extensively distributed to peripheral tissues because of a relatively lower tissue/blood partition coefficient of microemulsion system as a propofol vehicle.[5]

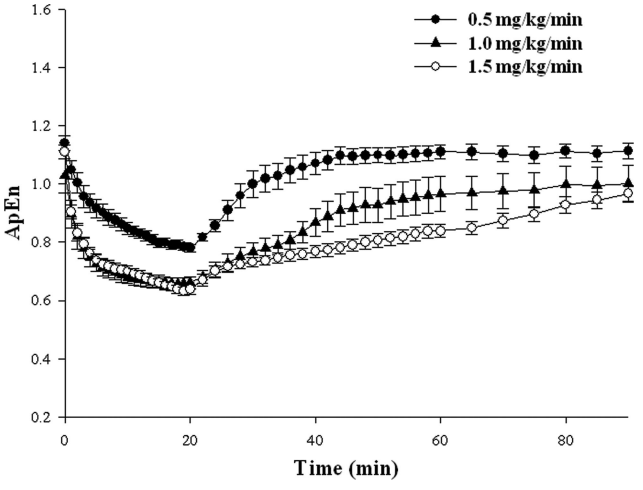

Fig. 6. The time course of the electroencephalographic entropy (ApEn) derived from the lateral left parietal cortex during and after the infusion of microemulsion propofol in rats. Data are stated as mean ± SE. *Solid circles* = ApEn at 0.5 mg · kg^{-1} · min^{-1}; *solid triangles* = ApEn at 1.0 mg · kg^{-1} · min^{-1}; *open circles* = ApEn at 1.5 mg · kg^{-1} · min^{-1}.

Table 5. Population Pharmacodynamic Parameter Estimates and Interindividual Variability (%CV) and Median Parameter Values (2.5–97.5%) of the Nonparametric Bootstrap Replicates of the Final Pharmacodynamic Model of a Reformulated Microemulsion Propofol

Parameter	Estimate (RSE, %CV)	Median	2.5–97.5%
E_0	1.18 (2.15, –)	1.18	1.12–1.22
E_{max}	0.636 (3.22, –)	0.636	0.596–0.676
Ce_{50}, μg/ml	1.87 (11.39, 62.4)	1.89	1.53–2.35
γ	1.28 (11.95, –)	1.30	1.03–1.63
k_{e0}, min^{-1}	1.02 (33.82, 86.3)	1.00	0.699–1.62
σ^2	0.0031 (11.8, –)	0.00301	0.0023–0.0037

Interindividual random variability and residual random variability were modeled using log-normal model and additive error model, respectively. Nonparametric bootstrap analysis was repeated 2,000 times.

Ce_{50} = effect site concentration of propofol that produces 50% of maximal effect on approximate entropy; CV = coefficient of variation; E_0 = baseline value of electroencephalographic approximate entropy; E_{max} = maximally decreased value of approximate entropy; γ = steepness of the concentration-*vs.*-response relation; σ^2 = variance of residual random variability; RSE = relative standard error.

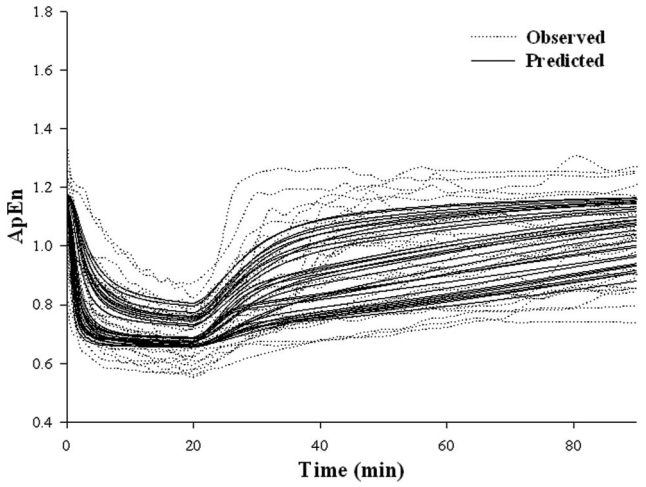

Fig. 7. Observed (*dotted line*) and predicted (*solid line*) electroencephalographic approximate entropy (ApEn) over time. The median absolute residual and its percentage of pharmacodynamic range ($E_0 - E_{max}$) of the final model were 0.056 and 10.33%, respectively.

Linear kinetic models permit the application of the superposition principle, in that doubling the dose will consequently lead to a doubling of the concentrations.[31] In this study, dose-normalized area under the curve was increased with increasing dose, suggesting nonlinear disposition, *i.e.*, a decrease in clearance. Propofol has a hepatic extraction ratio of nearly 0.8, and hepatic clearance accounts for a majority of the total propofol clearance.[41] Propofol reduces its own clearance with an increasing dose by reducing cardiac output and hepatic blood flow. The larger decrease in MAP at 1.0 and 1.5 mg · kg^{-1} · min^{-1} (−23% and −35% *vs.* baseline MAP) compared with 0.5 mg · kg^{-1} · min^{-1} (−4% *vs.* baseline MAP) in our study could potentially reduce hepatic perfusion and alter the pharmacokinetic profile of microemulsion propofol.

To describe nonlinear pharmacokinetics of a drug with high hepatic extraction ratio such as propofol, Michaelis-Menten elimination may be inappropriate, because it assumes that metabolism and/or renal secretion usually approach the capacity of the elimination system and the elimination rate is no longer strictly a constant.[31] The well-stirred model, also called the venous equilibrium model, may be more appropriate to describe nonlinear kinetics caused by changes in the perfusion of the liver.[31] The failure to fit the well-stirred model to pharmacokinetic data in this study may be attributed to either the small size of sample or insufficient and/or inhomogeneous decrease of MAP and hence hepatic blood flow, which may be supported by the large SDs of MAP at the infusion rates of 1.0 and 1.5 mg · kg^{-1} · min^{-1}. For highly cleared drugs, also called high-extraction compounds (hepatic extraction ratio ≥ 0.7), $f_u \cdot Cl_{int}$ in equation 3 is much greater than Q_H, and then $f_u \cdot Cl_{int}$ cancels out, which means that hepatic clearance is nearly equal to hepatic perfusion rate.[42] When assuming this for simplicity at the circumstance that hepatic blood flow is unknown or cannot be expressed as a function of MAP, the well-stirred model in this study is not distinguished mathematically from the two-compartment model with linear pharmacokinetics.

When discussing nonlinear kinetics, the relevant dose range should be considered because nearly every drug can have nonlinearity at an extreme dose. The infusion rates used in this study are comparable to the doses used in the studies for LCT propofol, in which the infusion rate of 0.5 to 1.3 mg · kg^{-1} · min^{-1} in rats can produce light anesthesia and deep anesthesia.[14,43,44] Because of the potential for nonlinear kinetics, caution should be taken when extrapolating the pharmacokinetic data in this study before making predictions regarding the pharmacokinetic behavior of microemulsion propofol at other doses in rats. However, the median weighted residual and median absolute weighted residual of the pharmacokinetic model in this study were comparable to those in a previous study using a two-compartment model with Michaelis-Menten elimination in rats, in which the median weighted residual and median absolute weighted residual were −1.6% and 30.5%, respectively.[14]

The estimates of γ and Ce_{50} of microemulsion propofol were lower than those of a previous study, in which modified median frequency was used as a surrogate measure of the effect of LCT propofol on the central nervous system.[14] Apparently, microemulsion propofol may be more potent than LCT propofol, and ApEn seemed to change less steeply than modified median frequency did. However, different surrogate measurement used for pharmacodynamic modeling might lead to different estimation of the pharmacodynamic parameters such as γ and Ce_{50}. Therefore, caution should be taken when comparing the results of both studies.

Because the placement of electroencephalographic electrodes in rats was not standardized, we selected and modified the methods that generally have been used in rat sleep research[29,45,46] and an epileptic model.[28] Although stainless steel electroencephalographic needle electrodes were placed occipito-occipitally in other studies,[16,47] the time course of ApEn in this study showed dose-dependent changes, suggesting the global effects of microemulsion propofol on the central nervous system in rats.

In conclusion, microemulsion propofol may have the potential to produce frequent and severe pain on injection because it contains higher concentrations of free propofol in the aqueous phase compared with those of the LCT propofol. Therefore, when microemulsion propofol is used in clinical settings, the techniques known to reduce pain on injection must be implemented. At the dose range used in this study, microemulsion propofol showed nonlinear pharmacokinetics,

which may be caused by the prominent hemodynamic depression.

The authors thank Ae-Kyung Hwang, B.S. (Technician), and Hyun-Jeong Park, B.S. (Technician), in the Clinical Research Center of Asan Medical Center (Seoul, Korea) for measurement of propofol concentrations.

References

1. Bennett SN, McNeil MM, Bland LA, Arduino MJ, Villarino ME, Perrotta DM, Burwen DR, Welbel SF, Pegues DA, Stroud L, Zeitz PS, Jarvis WR: Postoperative infections traced to contamination of an intravenous anesthetic, propofol. N Engl J Med 1995; 333:147–54

2. Park JW, Park ES, Chi SC, Kil HY, Lee KH: The effect of lidocaine on the globule size distribution of propofol emulsions. Anesth Analg 2003; 97:769–71

3. Devlin JW, Lau AK, Tanios MA: Propofol-associated hypertriglyceridemia and pancreatitis in the intensive care unit: An analysis of frequency and risk factors. Pharmacotherapy 2005; 25:1348–52

4. Yamakage M, Iwasaki S, Satoh J, Namiki A: Changes in concentrations of free propofol by modification of the solution. Anesth Analg 2005; 101:385–8

5. Kim KM, Choi BM, Park SW, Lee SH, Christensen LV, Zhou J, Yoo BH, Shin HW, Bae KS, Kern SE, Kang SH, Noh GJ: Pharmacokinetics and pharmacodynamics of propofol microemulsion and lipid emulsion after an intravenous bolus and variable rate infusion. ANESTHESIOLOGY 2007; 106:924–34

6. Ballas SK, Files B, Luchtman-Jones L, Benjamin L, Swerdlow P, Hilliard L, Coates T, Abboud M, Wojtowicz-Praga S, Grindel JM: Safety of purified poloxamer 188 in sickle cell disease: Phase I study of a non-ionic surfactant in the management of acute chest syndrome. Hemoglobin 2004; 28:85–102

7. Dubey PK, Kumar A: Pain on injection of lipid-free propofol and propofol emulsion containing medium-chain triglyceride: A comparative study. Anesth Analg 2005; 101:1060–2

8. Scott RP, Saunders DA, Norman J: Propofol: Clinical strategies for preventing the pain of injection. Anaesthesia 1988; 43:492–4

9. Iwama H, Nakane M, Ohmori S, Kaneko T, Kato M, Watanabe K, Okuaki A: Nafamostat mesilate, a kallikrein inhibitor, prevents pain on injection with propofol. Br J Anaesth 1998; 81:963–4

10. Song D, Hamza M, White PF, Klein K, Recart A, Khodaparast O: The pharmacodynamic effects of a lower-lipid emulsion of propofol: A comparison with the standard propofol emulsion. Anesth Analg 2004; 98:687–91

11. Klement W, Arndt JO: Pain on injection of propofol: Effects of concentration and diluent. Br J Anaesth 1991; 67:281–4

12. Soltesz S, Silomon M, Graf G, Mencke T, Boulaadass S, Molter GP: Effect of a 0.5% dilution of propofol on pain on injection during induction of anesthesia in children. ANESTHESIOLOGY 2007; 106:80–4

13. Brazeau GA, Cooper B, Svetic KA, Smith CL, Gupta P: Current perspectives on pain upon injection of drugs. J Pharm Sci 1998; 87:667–77

14. Ihmsen H, Tzabazis A, Schywalsky M, Schwilden H: Propofol in rats: Testing for nonlinear pharmacokinetics and modelling acute tolerance to EEG effects. Eur J Anaesthesiol 2002; 19:177–88

15. Hiraoka H, Yamamoto K, Okano N, Morita T, Goto F, Horiuchi R: Changes in drug plasma concentrations of an extensively bound and highly extracted drug, propofol, in response to altered plasma binding. Clin Pharmacol Ther 2004; 75:324–30

16. Ihmsen H, Schywalsky M, Tzabazis A, Schwilden H: Development of acute tolerance to the EEG effect of propofol in rats. Br J Anaesth 2005; 95:367–71

17. Bruhn J, Bouillon TW, Hoeft A, Shafer SL: Artifact robustness, inter- and intraindividual baseline stability, and rational EEG parameter selection. ANESTHESIOLOGY 2002; 96:54–9

18. Bruhn J, Ropcke H, Hoeft A: Approximate entropy as an electroencephalographic measure of anesthetic drug effect during desflurane anesthesia. ANESTHESIOLOGY 2000; 92:715–26

19. Bruhn J, Ropcke H, Rehberg B, Bouillon T, Hoeft A: Electroencephalogram approximate entropy correctly classifies the occurrence of burst suppression pattern as increasing anesthetic drug effect. ANESTHESIOLOGY 2000; 93:981–5

20. Baker MT, Gregerson MS, Martin SM, Buettner GR: Free radical and drug oxidation products in an intensive care unit sedative: propofol with sulfite. Crit Care Med 2003; 31:787–92

21. Tan LH, Hwang NC: The effect of mixing lidocaine with propofol on the dose of propofol required for induction of anesthesia. Anesth Analg 2003; 97:461–4

22. Koo SW, Cho SJ, Kim YK, Ham KD, Hwang JH: Small-dose ketamine reduces the pain of propofol injection. Anesth Analg 2006; 103:1444–7

23. Fujii Y, Uemura A: Effect of metoclopramide on pain on injection of propofol. Anaesth Intensive Care 2004; 32:653–6

24. Ambesh SP, Dubey PK, Sinha PK: Ondansetron pretreatment to alleviate pain on propofol injection: A randomized, controlled, double-blinded study. Anesth Analg 1999; 89:197–9

25. Agarwal A, Ansari MF, Gupta D, Pandey R, Raza M, Singh PK, Shiopriye, Dhiraj S, Singh U: Pretreatment with thiopental for prevention of pain associated with propofol injection. Anesth Analg 2004; 98:683–6

26. Cheong MA, Kim KS, Choi WJ: Ephedrine reduces the pain from propofol injection. Anesth Analg 2002; 95:1293–6

27. Shimamoto K, Iimura O: Measurement of circulating kinins, their changes by inhibition of kininase II and their possible blood pressure lowering effect. Agents Actions Suppl 1987; 22:297–307

28. D'Ambrosio R, Fairbanks JP, Fender JS, Born DE, Doyle DL, Miller JW: Post-traumatic epilepsy following fluid percussion injury in the rat. Brain 2004; 127:304–14

29. Pollock MS, Mistlberger RE: Rapid eye movement sleep induction by microinjection of the GABA-A antagonist bicuculline into the dorsal subcoeruleus area of the rat. Brain Res 2003; 962:68–77

30. Smith BP, Vandenhende FR, DeSante KA, Farid NA, Welch PA, Callaghan JT, Forgue ST: Confidence interval criteria for assessment of dose proportionality. Pharm Res 2000; 17:1278–83

31. Gabrielsson J, Weiner D: Pharmacokinetic concepts, Pharmacokinetic/Pharmacodynamic Data Analysis: Concepts and Applications. Edited by Gabrielsson J, Weiner D. Stockholm, Swedish Pharmaceutical Press, 2000, pp 45–174

32. Noh GJ, Kim KM, Jeong YB, Jeong SW, Yoon HS, Jeong SM, Kang SH, Linares O, Kern SE: Electroencephalographic approximate entropy changes in healthy volunteers during remifentanil infusion. ANESTHESIOLOGY 2006; 104:921–32

33. Beal S, Sheiner L: NONMEM User's Guides Part V: Introductory Guide. San Francisco, NONMEM Project Group, University of California, 1992, p 48

34. Shapiro SS, Wilk MB, Chen HJ: A comparative study of various tests for normality. J Am Stat Assoc 1968; 63:1343–72

35. Royston P: Estimating departure from normality. Stat Med 1991; 10:1283–93

36. Parke J, Holford NH, Charles BG: A procedure for generating bootstrap samples for the validation of nonlinear mixed-effects population models. Comput Methods Programs Biomed 1999; 59:19–29

37. Ohmizo H, Obara S, Iwama H: Mechanism of injection pain with long and long-medium chain triglyceride emulsive propofol. Can J Anaesth 2005; 52:595–9

38. Nakane M, Iwama H: A potential mechanism of propofol-induced pain on injection based on studies using nafamostat mesilate. Br J Anaesth 1999; 83:397–404

39. Klement W, Arndt JO: Pain on i. Br J Anaesth 1991; 66:189–95

40. Tan CH, Onsiong MK: Pain on injection of propofol. Anaesthesia 1998; 53:468–76

41. Lange H, Stephan H, Rieke H, Kellermann M, Sonntag H, Bircher J: Hepatic and extrahepatic disposition of propofol in patients undergoing coronary bypass surgery. Br J Anaesth 1990; 64:563–70

42. Wilkinson GR, Shand DG: Commentary: A physiological approach to hepatic drug clearance. Clin Pharmacol Ther 1975; 18:377–90

43. Yang CH, Shyr MH, Kuo TB, Tan PP, Chan SH: Effects of propofol on nociceptive response and power spectra of electroencephalographic and systemic arterial pressure signals in the rat: correlation with plasma concentration. J Pharmacol Exp Ther 1995; 275:1568–74

44. Cox EH, Knibbe CA, Koster VS, Langemeijer MW, Tukker EE, Lange R, Kuks PF, Langemeijer HJ, Lie AHL, Danhof M: Influence of different fat emulsion-based intravenous formulations on the pharmacokinetics and pharmacodynamics of propofol. Pharm Res 1998; 15:442–8

45. Mistlberger RE, Bergmann BM, Rechtschaffen A: Relationships among wake episode lengths, contiguous sleep episode lengths, and electroencephalographic delta waves in rats with suprachiasmatic nuclei lesions. Sleep 1987; 10:12–24

46. Mistlberger RE, Bergmann BM, Waldenar W, Rechtschaffen A: Recovery sleep following sleep deprivation in intact and suprachiasmatic nuclei-lesioned rats. Sleep 1983; 6:217–33

47. Schywalsky M, Ihmsen H, Tzabazis A, Fechner J, Burak E, Vornov J, Schwilden H: Pharmacokinetics and pharmacodynamics of the new propofol prodrug GPI 15715 in rats. Eur J Anaesthesiol 2003; 20:182–90